Connectivity and limitation of critical current in Bi-Pb-Sr-Ca-Cu/Ag tapes

K.-H. Müller, C. Andrikidis, J. Du, K. E. Leslie, and C. P. Foley
CSIRO, Telecommunications and Industrial Physics, Lindfield, Australia 2070
(Received 4 May 1998)

We have shown experimentally that the remanent magnetic moments of Y-Ba-Cu-O thin-film networks and of Bi-2223/Ag monofilamentary tapes show remarkable similarities, as their magnetic moments are both composed of intersquare (intergrain) and intrasquare (intragrain) magnetic moments. Starting from the geometrical definition of connectivity in a thin-film network, we show that connectivity in a Bi-2223/Ag monofilamentary tape is solely defined by the ratio of the average grain size to the width of the superconducting core and by the ratio of the intergrain to intragrain remanent magnetic moments at saturation. The measured upper limit for the connectivities ranged from 4.2×10^{-3} in a tape with low critical current density J_c to 2.9 $\times10^{-2}$ in a tape with $J_c(77\,\mathrm{K},0\,\mathrm{T})\simeq2\times10^{8}\,\mathrm{A\,m^{-2}}$. Our study reveals that even good Bi-2223/Ag tapes suffer from very low grain connectivity. We estimate that in the case of perfect connectivity a $J_c(77\,\mathrm{K},0\,\mathrm{T})$ between 8×10^{9} and $6\times10^{10}\,\mathrm{A\,m^{-2}}$ would be achievable. [S0163-1829(99)03925-9]

I. INTRODUCTION

Monofilamentary and multifilamentary silver-clad Bi-Pb-Sr-Ca-Cu (Bi-2223/Ag) tapes of kilometer length have been fabricated[1] using the powder-in-tube method where a high *c*-axis alignment of grains in the filaments is achieved by a combination of pressing, rolling and heating.[2–4] The critical current density reached is typically $2\times10^{8}\,\mathrm{A\,m^{-2}}$ at a temperature of 77 K in self-field, though short pieces of some tapes[5,6] show critical current densities higher than $6\times10^{8}\,\mathrm{A\,m^{-2}}$. These encouragingly high critical current densities have led to the fabrication of prototype power cables, magnets and motors.[7,8]

The grains in a superconducting filament of Bi-2223/Ag tapes have the shape of small platelets with large aspect ratios of typically less than 1 μm thickness in the *c* direction and an average diameter of about 20 μm in the *a* and *b* directions.[9,10] The platelets generally align within 5°–10° of the *c* direction of the tape,[11] and the *a* and *b* directions are oriented at random from platelet to platelet. The grains are connected by grain boundaries at different misalignment angles, and there are often voids between grains.[12] Because of the small coherence length in the Bi-2223 material, grain boundaries act as Josephson weak links if the misalignment angle is greater than about 5°.[13] This is very different in low-temperature superconductors where the coherence length is larger by about a factor of 10 and grain boundaries do not generally act as weak links.

The critical current of a granular high-temperature superconductor such as the Bi-2223/Ag tape is determined by two independent factors. The first factor is the grain connectivity and the second the critical current density in the grains associated with flux line pinning. In this paper, we first define the connectivity *C* and then show results of connectivity measurements. In Sec. II we introduce connectivity for the case of a thin-film network where *C* can be defined based on the geometry of the network. In Sec. III we define an equivalent connectivity for a Bi-2223/Ag monofilamentary tape. In Sec. IV we describe some experimental details, and in Sec. V we discuss the measured connectivities of two thin-film networks and of three different monofilamentary Bi-2223/Ag tapes. The very low connectivity in the Bi-2223/Ag tapes we examined reveals that granularity strongly limits the transport current density.

II. DEFINITION OF CONNECTIVITY IN A THIN-FILM NETWORK

Let us first consider a superconducting thin-film network of $n\times n$ squares with $n\gg1$. Each square has a width of $2s$, and the squares are joined by bridges of width *b* and length *h*. The thickness of the thin film is *d*. A network of this type is shown in Fig. 1. The connectivity *C* of such a network can be defined in geometrical terms as the ratio of the bridge

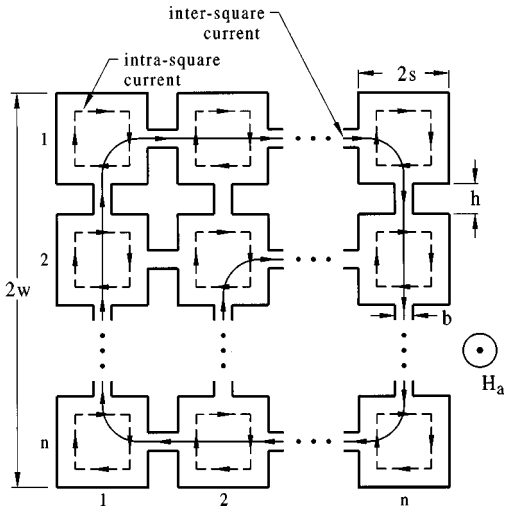

FIG. 1. $n\times n$ Y-Ba-Cu-O (YBCO) thin-film square array network where squares of width $2s$ are joined by bridges of width *b* and length *h*. A magnetic field H_a is applied perpendicular to the network. Schematically shown are the induced concentric intersquare currents (full line) which circulate over the full array while intrasquare currents (dashed line) circulate inside the squares. When after zero-field cooling the field H_a is increased, intersquare and intrasquare critical currents circulate clockwise.

width b to the sum of square-width $2s$ and gap width h, i.e.,

$$C=\frac{b}{2s+h}. \tag{1}$$

In the case where the bridge width b is zero, the connectivity is zero as squares are fully separated by gaps, while for $b=2s$ and $h=0$ the connectivity is maximal, i.e., $C=1$.

In the case of a superconducting thin-film network of this kind, the intersquare critical current density J_c^I is given by

$$J_c^I=\frac{b}{2s+h}J_c \tag{2}$$

or, equivalently,

$$J_c^I=CJ_c, \tag{3}$$

where J_c is the critical current density of the superconducting thin film, i.e., J_c is the intrasquare critical current density. Equations (1) and (3) show that C is determined by the geometry of the network or, alternatively, by the ratio of the intersquare to intrasquare critical current densities.

One way to obtain J_c^I and J_c is to determine the magnitudes of the intersquare and intrasquare remanent magnetic moments, $m_{R,s}^I$ and $m_{R,s}^G$ at saturation. Let us assume that after zero-field cooling an increasing magnetic field H_a is applied perpendicular to a thin-film network such as the one shown in Fig. 1 and that $H_{c1}\ll H_a$ where H_{c1} is the lower critical field of the thin film. An intersquare current will be induced as schematically indicated in Fig. 1 (clockwise flow direction) and will gradually reach its critical current value of $I_c^b=bdJ_c$. Intersquare currents first saturate in the outer bridges, and with increasing applied field, current saturation moves inwards. When the applied field is decreased from its maximum value H_m, the intersquare currents start flowing in the opposite direction (counterclockwise in Fig. 1), a process which starts from the outside and moves inwards while the field decreases. At zero field the intersquare currents produce the intersquare remanent magnetic moment. Saturation of the intersquare remanent magnetic moment m_R^I is achieved by applying a sufficiently high field such that after returning to zero field, the maximum intersquare current I_c^b is flowing in the opposite direction in all bridges. While the applied field is increased, intrasquare currents are induced in the squares. Here the process of saturation is similar to that of the intersquare moment. Saturation of the intrasquare remanent magnetic moment m_R^G is achieved by applying a sufficiently high field such that after decreasing the field to zero, the intrasquare current is at its maximum value of $I_c^G=sdJ_c$ [assuming $b\ll(2s+h)$] and is flowing in opposite direction (counterclockwise) in all squares. The sum of the intersquare and intrasquare remanent moments m_R^I and m_R^G is the total remanent magnetic moment m_R. If there are no bridges between the squares, currents will be induced in all squares without any shielding effects from intersquare currents.

Using the definition of the magnetic moment **m**, where

$$\mathbf{m}=\frac{1}{2}\int \mathbf{r}\times\mathbf{J}(\mathbf{r})d^3r \tag{4}$$

[**r** is the spatial vector and $\mathbf{J}(\mathbf{r})$ the current density at point **r**) one obtains for the intersquare remanent magnetic moment in a perpendicular applied field H_a (see Fig. 1) at saturation ($H_a\to\infty$)

$$m_{R,s}^I=\frac{4}{3}w^3dCJ_c. \tag{5}$$

Here, w is the half width of the network array (see Fig. 1) and d the thickness of the film. The intrasquare remanent magnetic moment $m_{R,s}^G$ at saturation, which originates from a thin-film array of squares without bridges is (Fig. 1 with $b=0$)

$$m_{R,s}^G=\left(\frac{2w}{2s+h}\right)^2\frac{4}{3}s^3dJ_c. \tag{6}$$

Here, the factor $[2w/(2s+h)]^2$ is the number of squares in the array and $4s^3dJ_c/3$ is the remanent magnetic moment at saturation of a single square of width $2s$ and thickness d.

From Eqs. (5) and (6) we derive for the connectivity C the expression

$$C=\frac{s^3}{w(s+h/2)^2}\frac{m_{R,s}^I}{m_{R,s}^G}. \tag{7}$$

The superconducting volume fraction f_s of the network in Fig. 1 is

$$f_s=\frac{s^2+hb/2}{(s+h/2)^2}. \tag{8}$$

Assuming $hb\ll 4s^2$, i.e., the bridge area is small compared to the area of a single square, one finds

$$C=f_s\frac{s}{w}\frac{m_{R,s}^I}{m_{R,s}^G}. \tag{9}$$

If $b\ll(2s+h)$ (small connectivity) one can use the fact that the total remanent magnetic moment, $m_{R,s}$, at saturation is given by

$$m_{R,s}=m_{R,s}^I+m_{R,s}^G, \tag{10}$$

which gives for the connectivity the expression

$$C=f_s\frac{s}{w}\left(\frac{m_{R,s}}{m_{R,s}^G}-1\right). \tag{11}$$

If the condition $b\ll(2s+h)$ does not hold, the expression for $m_{R,s}^G$ of Eq. (6) has to be modified by including the intersquare current which flows through each square which will lead to a smaller $m_{R,s}^G$.

III. DEFINITION OF CONNECTIVITY IN A Bi-2223/Ag TAPE

In order to determine the connectivity C of a Bi-2223/Ag monofilamentary tape, we use Eq. (3) and define

$$C=\frac{J_c^I}{J_c}. \tag{12}$$

Using Eq. (4) one derives for the intergrain remanent magnetic moment at saturation in a perpendicular field

$$m_{R,s}^{I}=DJ_c^{I}\left(La^2-\frac{2}{3}a^3\right), \tag{13}$$

where L is the length of the tape, D the average thickness of the superconducting core, a the half width of the core, and J_c^I the intergrain critical current density (transport critical current density) of the tape.

Assuming that the grains in the tape are thin platelets of average radius R_G and that the applied field is perpendicular to the platelets, one derives for the intragrain remanent magnetic moment $m_{R,s}^{G}$ at saturation

$$m_{R,s}^{G}=\frac{2}{3}f_s aDLR_G J_c. \tag{14}$$

f_s is the superconducting volume fraction and J_c the intragrain critical current density. From Eqs. (12), (13), and (14) one obtains for the connectivity C of a Bi-2223/Ag monofilamentary tape

$$C=\frac{2}{3}f_s\frac{R_G}{a(1-2a/3L)}\frac{m_{R,s}^{I}}{m_{R,s}^{G}}. \tag{15}$$

Or if $C\ll 1$,

$$C=\frac{2}{3}\frac{R_G}{a(1-2a/3L)}\left(\frac{m_{R,s}}{m_{R,s}^{G}}-1\right), \tag{16}$$

where Eq. (10) has been used. Equation (15) is very similar to Eq. (9) where Eq. (9) can be obtained from Eq. (15) by setting $L=2a$ (square shaped superconducting core) and using $R_G\rightarrow s$ and $a\rightarrow w$.

It is not surprising that Eqs. (15) and (9) are similar. In a simplistic picture, the core of a Bi-2223/Ag tape can be viewed as an array as in Fig. 1 where s represents the average radius R_G of the grain platelets in the core and b the average width of strong links. The gap h in Fig. 1 is a measure of the void content. A somewhat improved picture would be to think of the core of a monofilamentary Bi-2223/Ag tape as being made up of thin layers of many networks such as the one shown in Fig. 1, stacked on top of each other, where the layers are insulated from each other but where the layers are not aligned. The thickness of a single layer would resemble the average thickness of the grain platelets. Interestingly, any random alignment has no effect on the values of $m_{R,s}^{I}$ and $m_{R,s}^{G}$ in a perpendicular applied field. An even more refined picture would be that of layered networks where R_G, b, and h are randomly chosen from the corresponding distributions found in Bi-2223/Ag tapes.

In the case of a thin-film network, connectivity can be defined solely in geometrical terms as was done in Eq. (1). In the case of a Bi-2223/Ag tape the situation is more complicated. Here bridges are thought to correspond to grain boundaries with a misalignment angle less than a certain critical angle Θ_c, which might be between 5^o and 10^o. For $\Theta<\Theta_c$ the Josephson critical current density J_c^{GB} of a grain boundary is greater than or equal to J_c, and the grain boundary acts as a strong link, similar to the bridges in a thin-film network. For $\Theta>\Theta_c$, J_c^{GB} drops rapidly with increasing Θ and the grain boundary no longer behaves as a bridge but more similar to a gap or a very weak link.[13] Therefore, in the case of a monofilamentary Bi-2223/Ag tape, connectivity measures the ratio of the projected area (in macroscopic current flow direction) of strong-link grain boundaries to the transverse cross-sectional area of the superconducting core. For a multifilamentary tape connectivity can be defined in a similar way.

It seems appealing to discuss an alternative way of determinating the connectivity C of a tape by measuring the intergrain characteristic field

$$H_D=J_c^{I}D/\pi \tag{17}$$

and to measure the average field of full penetration H^* of the grains where H^* is proportional to J_c. H_D can be determined by measuring the remanent intergrain magnetic moment m_R^I as a function of the maximum applied field H_m as follows. According to Ref. 14, m_R^I of a superconducting strip $(D\ll a\ll L)$ can be written as

$$m_R^I=-\pi a^2 LH_D\left[\tanh\xi-2\tanh\frac{\xi}{2}\right], \tag{18}$$

where $\xi=H_m/H_D$. Using Eq. (18), one can show that $dm_R^I/d(\log_{10}H_m)$ has a maximum at $H_m=H_m^I$ where

$$H_m^I=1.9687H_D. \tag{19}$$

If one assumes that the grains in the tape are stacked on top of each other (along the c direction) and thus mutually shield each other, one can approximately describe the grains as cylinders of average radius R_G and length D, with the cylinder axis in the c direction and a demagnetizing factor close to 0. Then

$$H^*=J_cR_G. \tag{20}$$

If on the other hand one approximates the grains by magnetically isolated, disklike platelets of radius R_G and thickness t, where $t\ll R_G$, then[15] the demagnetizing factor approaches 1, and one has

$$H^*=J_ct/2. \tag{21}$$

Depending on which case is realized, H^* can be determined by measuring m_R^G as a function of H_m as follows. Approximating the grains in the tape by long cylinders of radius R_G and length D where $D\gg R_G$, one finds for the intragrain remanent magnetic moment[16,17]

$$m_R^G=2f_saLDH^*\begin{cases}\frac{1}{2}\eta^2-\frac{1}{4}\eta^3, & 0\leqslant\eta\leqslant 1,\\ -\frac{1}{3}+\eta-\frac{1}{2}\eta^2+\frac{1}{12}\eta^3, & 1\leqslant\eta\leqslant 2,\\ \frac{1}{3}, & \eta\geqslant 2,\end{cases} \tag{22}$$

where $\eta=H_m/H^*$ and $H^*=R_GJ_c$.

Using Eq. (22), one can show that $dm_R^G/d(\log_{10} H_m)$ has a maximum at $H_m = H_m^G$, where

$$H_m^G = 0.8889 H^*. \tag{23}$$

From Eqs. (12), (17), (19), (20), and (23) one obtains

$$C = \frac{0.8889}{1.9687}\pi \frac{R_G}{D}\frac{H_m^I}{H_m^G}. \tag{24}$$

Alternatively, approximating the grains of the tape by thin platelets of radius R_G and thickness t, one finds for the intergrain remanent magnetic moment[15,16]

$$m_R^G = f_s \frac{4aLD}{3\pi} J_c R_G \left[-\arccos\left(\frac{1}{\cosh \eta}\right) - \frac{\sinh \eta}{\cosh^2 \eta} + 2\arccos\left(\frac{1}{\cosh(\eta/2)}\right) + 2\frac{\sinh(\eta/2)}{\cosh^2(\eta/2)}\right], \tag{25}$$

where $\eta = H_m/H^*$ with $H^* = J_c t/2$. Using Eq. (25), one can show that $dm_R^G/d(\log_{10} H_m)$ has a maximum at $H_m = H_m^G$, where

$$H_m^G = 1.5425 H^*. \tag{26}$$

From Eqs. (12), (17), (19), (21), and (26) one obtains

$$C = \frac{1.5425}{1.9687}\frac{\pi}{2}\frac{t}{D}\frac{H_m^I}{H_m^G}. \tag{27}$$

Equation (27) differs from Eq. (24) in that it contains the factor t/D instead of R_G/D. In a Bi-2223/Ag tape, $t < 1\ \mu$m, and thus $t \ll R_G$. Equations (27) and (24) were derived under extreme assumptions about the demagnetizing factor of the grains which lead to rather different expressions for C. This clearly suggests that trying to determine the connectivity C from H_D and H^* is not suitable as the relationship between H^* and J_c is not sufficiently well known. In contrast, the intragrain magnetic moment at saturation is totally independent of any assumption about the demagnetizing effect of grains. For $H_m \gg H^*$ (saturation) one obtains from Eq. (22) as well as from Eq. (25) the expression $m_{R,s}^G = 2 f_s aDLR_G J_c/3$, which is Eq. (14). Therefore, the connectivity C of a monofilamentary Bi-2223/Ag tape should be determined by using Eq. (15) where $m_{R,s}^I$ and $m_{R,s}^G$ enter, and not from Eqs. (24) or (27) where H^* enters.

IV. EXPERIMENT

High quality YBCO/MgO thin films were patterned into arrays of $n \times n$ squares with and without joining bridges. A $n \times n$ network with bridges is shown in Fig. 1 where the total width of the array is $2w$, the width of a square is $2s$, the bridge width b, and its length h. Four arrays were produced, two arrays with $n = 16$, one with and one without bridges, and two arrays with $n = 28$, one with and one without bridges. Table I shows the values of n, w, s, b, and h for the two different networks. The thin films all had a thickness of $d \simeq 0.3\ \mu$m. The film J_c (intrasquare J_c) was determined magnetically and was found to be about 2×10^{10} A m^{-2} at 77 K. The remanent magnetic moments of these four arrays were measured as a function of the maximum magnetic field $H_a = H_m$, applied perpendicular to the thin-film surface (see Fig. 1), using a Quantum Design superconducting quantum interference device (SQUID) magnetometer. A 5-cm scan was used, and the field was swept in the no-overshoot mode. The temperature chosen was 5 K and the highest field applied was 5.5 T.

TABLE I. Values for n, w, s, b, and H (see Fig. 1) for the two different YBCO thin-film networks. Values for the connectivity C were obtained using Eqs. (1) and (9).

n	w [μm]	s [μm]	b [μm]	h [μm]	C [Eq. (1)]	C [Eq. (9)]
16	1451	86	10	10	0.055	0.058
28	1474	43	10	20	0.094	0.085

The same type of measurements was performed on three short samples of Bi-2223/Ag monofilamentary tapes (tapes 1–3), prepared by Dou *et al.*, employing the powder-in-tube method.[4] Microstructural investigations and critical current measurements as a function of temperature and magnetic field showed that the monofilamentary tapes were similar to tapes prepared by other groups.[12] The tapes' half width a and length L together with the electrically measured transport critical current density $J_c^{\rm trans}(77\,{\rm K},0\,{\rm T})$, are listed in Table II. Tape 1 had the lowest $J_c^{\rm trans}(77\,{\rm K},0\,{\rm T})$ of about 2×10^7 A m^{-2} while tape 3 had the highest $J_c^{\rm trans}(77\,{\rm K},0\,{\rm T})$ of about 2×10^8 A m^{-2}. First, the remanent magnetic moments m_R of the three intact tapes were measured. Then, the tapes were severely bent (rolled) to the small diameter of about 1.5 mm. After straightening the tapes, their remanent moments m_R^G were measured.[18–20] The idea is that severe bending creates a large number of microcracks, preventing an intergrain current to flow over the whole superconducting core. The observed average spacing between these cracks was found to be about 100 μm.[21] Calculations show that the total intergrain magnetic moment resulting from these 100 μm wide grain clusters is small compared with the total intragrain magnetic moment originating from individual grains. There-

TABLE II. Values for the transport critical current density $J_c^{\rm trans}$(77 K, 0 T) average thickness D, core half width a, and length L of the three monofilamentary Bi-2223/Ag tapes. Values for the ideal minimal and maximal transport critical current densities $\tilde{J}_{c,\rm min}^{\rm trans}$ and $\tilde{J}_{c,\rm max}^{\rm trans}$ defined below are also given.

tape	$J_c^{\rm trans}$(77 K, 0 T) [A m^{-2}]	D [μm]	a [mm]	L [mm]	$\tilde{J}_{c,\rm min}^{\rm trans}$ [A m^{-2}]	$\tilde{J}_{c,\rm max}^{\rm trans}$ [A m^{-2}]
1	$\sim 2 \times 10^7$	40	1.6	5.9	9.4×10^9	5.9×10^{10}
2	$\sim 5 \times 10^7$	65	1.6	6.2	8.2×10^9	5.2×10^{10}
3	$\sim 2 \times 10^8$	60	1.3	5.8	9.2×10^9	5.8×10^{10}

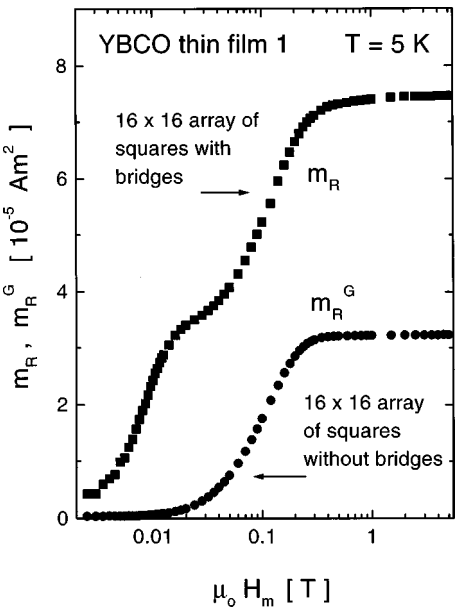

FIG. 2. Total remanent magnetic moment m_R of a 16 $\times$16 YBCO array with bridges and the intrasquare remanent magnetic moment m_R^G of the same 16$\times$16 YBCO array without bridges versus the maximum field H_m at $T=5$ K.

fore, the remanent magnetic moment measured after severe bending is m_R^G, the intragrain remanent magnetic moment.[22]

V. RESULTS AND DISCUSSION

Figure 2 shows the remanent magnetic moment m_R of the 16$\times$16 array of squares with bridges and the remanent magnetic moment m_R^G of the 16$\times$16 array without bridges, as a function of the maximum applied magnetic field H_m. The m_R data show a knee at $\mu_0 H_m \simeq 0.02$ T and saturation at

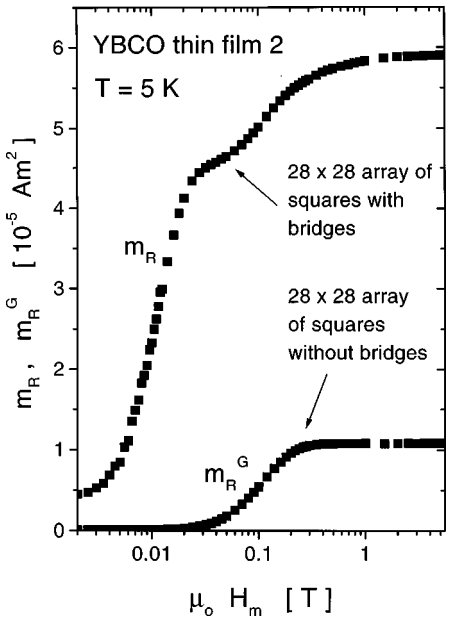

FIG. 3. Total remanent magnetic moment m_R of a 28 $\times$28 YBCO array with bridges and the intrasquare remanent magnetic moment m_R^G of the same 28$\times$28 YBCO array without bridges versus the maximum field H_m at $T=5$ K.

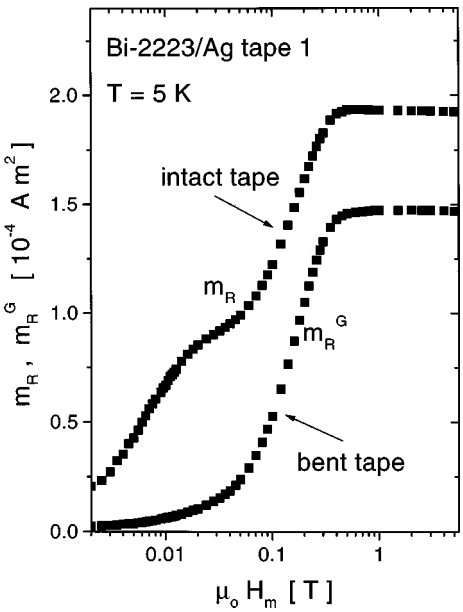

FIG. 4. Total remanent magnetic moment m_R of the intact Bi-2223/Ag tape 1 and the intragrain (bent tape) remanent magnetic moment m_R^G versus the maximum field H_m at $T=5$ K.

$\mu_0 H_m \geqslant 0.3$ T. The knee is due to the saturation of the intersquare currents and thus $m_R(\text{knee}) = m_{R,s}^I$. The saturation above 0.3 T is due to the saturation of the intrasquare currents. The m_R^G data shows saturation at $\mu_0 H_m \geqslant 0.3$ T, in agreement with the m_R data.

Figure 3 shows m_R and m_R^G for the 28$\times$28 array. The $m_{R,s}^I/m_{R,s}^G$ ratio is larger than in the case of the 16$\times$16 array which is mainly due to the smaller squares in the 28$\times$28 array (Table I). From the data in Figs. 2 and 3 one can see that $m_R(H_m \to \infty) \simeq m_{R,s}^I + m_{R,s}^G$. Table I shows values for the connectivity C using Eq. (1) with the listed values for s, b,

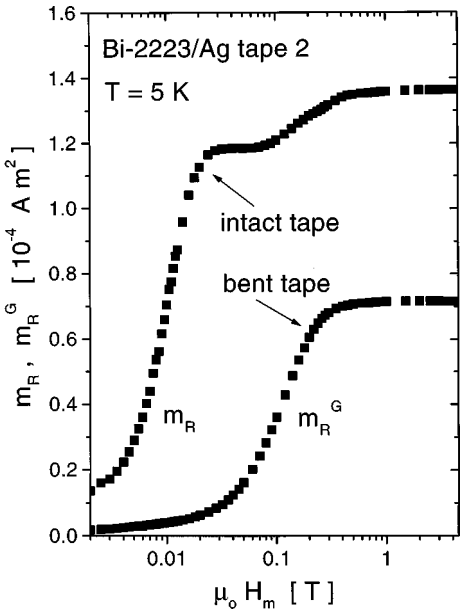

FIG. 5. Total remanent magnetic moment m_R of the intact Bi-2223/Ag tape 2 and the intragrain (bent tape) remanent magnetic moment m_R^G versus the maximum field H_m at $T=5$ K.

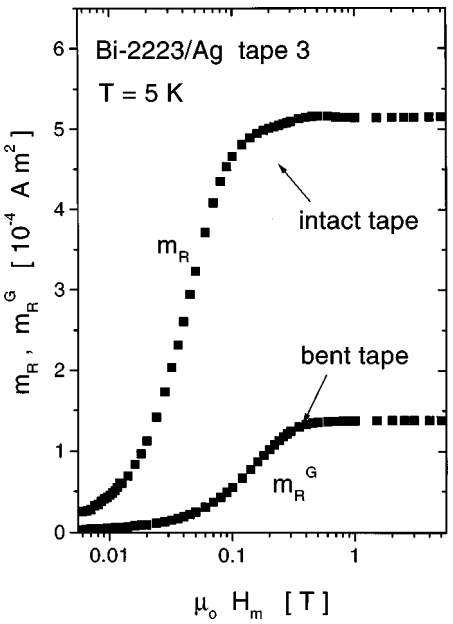

FIG. 6. Total remanent magnetic moment m_R of the intact Bi-2223/Ag tape 3 and the intragrain (bent tape) remanent magnetic moment m_R^G versus the maximum field H_m at $T=5$ K.

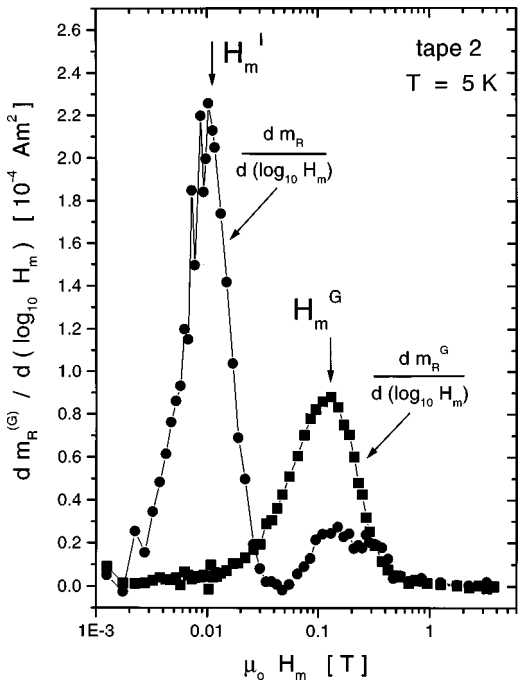

FIG. 7. Derivatives $dm_R/d(\log_{10}H_m)$ (dots) and $dm_R^G/d(\log_{10}H_m)$ (squares) versus H_m for the Bi-2223/Ag tape 2 at $T=5$ K. The fields H_m^I [Eq. (19)] and H_m^G [Eq. (26)] are indicated.

and h. Also shown in Table I are connectivities C using Eq. (9) with data for $m_{R,s}^I$ and $m_{R,s}^G$ from Figs. 2 and 3. The connectivities determined from the magnetic moments [Eq. (9)] agree reasonably well with the geometrically determined connectivities [Eq. (1)].

Table II lists for the three different monofilamentary Bi-2223/Ag tapes the measured transport critical current densities $J_c^{\rm trans}(77\,{\rm K},0\,{\rm T})$, the average thickness D, the core half width a, and the length L. Figures 4–6 show the total remanent magnetic moments m_R and the intragrain remanent magnetic moment m_R^G versus the maximum applied magnetic field H_m for the monofilamentary Bi-2223/Ag tapes 1–3. It is important to note that the m_R and m_R^G data of the tapes strongly resemble those of the thin-film arrays displayed in Figs. 2 and 3. As seen in Fig. 4, tape 1, which has the lowest $J_c^{\rm trans}$, exhibits the lowest $m_{R,s}^I/m_{R,s}^G$ ratio. Tape 2 in Fig. 5 shows a well developed knee at $\mu_0 H_m \simeq 0.03\,{\rm T}$ due to a larger intergrain critical current density. Figure 6 shows m_R and m_R^G versus H_m for tape 3 which has the highest $J_c^{\rm trans}$. Here the knee has moved to an H_m value close to where m_R^G saturates, causing the signature of the knee to disappear almost completely.

It is important to notice that in Figs. 4–6, $m_R(H_m\to\infty) < m_{R,s}^I + m_{R,s}^G$ where $m_{R,S}^I = m_R$(knee), in contrast to Figs. 2 and 3. The fact that $m_R(H_m\to\infty) < m_{R,s}^I + m_{R,s}^G$ is caused by the hysteretic behavior of J_c^I where flux trapped in the grains significantly reduces J_c^I for $H_m > H_{c1G}$ (H_{c1G} is the lower critical field of the grains) as has been discussed in Ref. 18.

In order to calculate the connectivity C of the three Bi-2223/Ag tapes from Eq. (15), values for f_s and R_G have to be chosen. We assume $0.7 \leqslant f_s \leqslant 0.9$ and $3\,\mu{\rm m} \leqslant R_G \leqslant 15\,\mu{\rm m}$ which seems a reasonable range estimate.[23] The uncertainties in f_s and R_G lead to an uncertainty in C where $C_{\rm min} \leqslant C \leqslant C_{\rm max}$, with $C_{\rm min}$ the connectivity with the smallest f_s and R_G and $C_{\rm max}$ the connectivity with the largest f_s and R_G. Table III lists besides $m_{R,s}^I$ and $m_{R,s}^G$ the results for $C_{\rm min}$ and $C_{\rm max}$ using Eq. (15). $C_{\rm min}$ ranges from 6.5×10^{-4} for tape 1 to 4.5×10^{-3} for tape 3 while $C_{\rm max}$ ranges from 4.2×10^{-3} to 2.9×10^{-2}. These are very small connectivities, implying that better grain connectivity would significantly improve the intergrain critical current density J_c^I and therefore the transport critical current density $J_c^{\rm trans}$. In Table III, values for $C_{\rm max}^{-1}$ and $C_{\rm min}^{-1}$ are also listed which represent the factors by which one could improve $J_c^{\rm trans}$ theoretically. $C_{\rm max}^{-1}$ ranges from 46 to 472 and $C_{\rm min}^{-1}$ from 290 to 3000. It is important to note that the range of the ideal transport current density, i.e., $\tilde{J}_{c,{\rm min(max)}}^{\rm trans} \equiv C_{\rm max(min)}^{-1} J_c^{\rm trans}$, listed in Table II, is almost the same for the three tapes with $8\times10^9\,{\rm A\,m^{-2}} < \tilde{J}_c^{\rm trans}(77\,{\rm K},0\,{\rm T}) < 6\times10^{10}\,{\rm A\,m^{-2}}$. This indicates that the

TABLE III. Values for the intergrain and intragrain remanent moments at saturation, $m_{R,s}^I$ and $m_{R,s}^G$ and the minimal and maximal connectivities $C_{\rm min}$ and $C_{\rm max}$, as well as their inverse values.

tape	$m_{R,s}^I$ [10^{-4} A m^2]	$m_{R,s}^G$ [10^{-4} A m^2]	$C_{\rm min}$ [Eq. (15)]	$C_{\rm max}$ [Eq. (15)]	$C_{\rm min}^{-1}$ [Eq. (15)]	$C_{\rm max}^{-1}$ [Eq. (15)]
1	0.9	1.47	0.00065	0.0042	2997	472
2	1.2	0.72	0.0018	0.0114	1035	163
3	5.0	1.38	0.0045	0.029	290	46

TABLE IV. Values for H_m^I and H_m^G (see Fig. 7) as well as connectivities $C_{\min}$ and $C_{\max}$ using Eq. (24) and C using Eq. (27) for the three monofilamentary Bi-2223/Ag tapes.

tape	H_m^I [mT]	H_m^G [mT]	$C_{\min}$ [Eq. (24)]	$C_{\max}$ [Eq. (24)]	C [Eq. (27)]
1	6.7	170	0.00419	0.02096	0.00121
2	10	130	0.00504	0.02518	0.00146
3	46	150	0.02175	0.10875	0.00629

intragrain current density J_c is about the same in the three tapes.

Finally, we report on values for C which are obtained using the less reliable estimates of Eqs. (24) and (27). The values for H_m^I and H_m^G are obtained from plots of $dm_R/d(\log_{10} H_m)$ and $dm_R^G/d(\log_{10} H_m)$ versus H_m which are shown in Fig. 7 for tape 2.[20] The values of H_m^I and H_m^G for the three different Bi-2223/Ag tapes are listed in Table IV together with $C_{\min}$ and $C_{\max}$ of Eq. (24) and C of Eq. (27) where $t=1$ μm was used. As expected, $C_{\min}$ and $C_{\max}$ of Eq. (24) are larger than the more reliable C values obtained from Eq. (15) while Eq. (27) delivers rather small values for C compared to Eq. (15).

The above determination of the connectivity C in monofilamentary Bi-2223/Ag tapes can in principal also be applied to multifilamentary Bi-22223/Ag tapes. In the case of multifilamentary tapes, Eqs. (13) and (14) for the intergrain and intragrain remanent magnetic moments at saturation $m_{R,s}^I$ and $m_{R,s}^G$, have to be modified accordingly by taking the geometry of the filaments into account. Because of the integral nature of $m_{R,s}^I$, it would be difficult to consider differences in J_c^I in different filaments as observed in Ref. 24. Because of the generally better grain alignment in multifilamentary tapes compared with monofilamentary ones, larger connectivity values can be expected for multifilamentary tapes.

VI. CONCLUSIONS

We have introduced a definition for the connectivity in monofilamentary tapes, starting from the geometrical definition of connectivity in a superconducting thin-film network of bridged squares. We have shown that in order to determine connectivity in a monofilamentary Bi-2223/Ag tape, the intergrain and intragrain magnetic moments at saturation have to be measured and the average grain radius and superconducting volume fraction have to be estimated. An alternative method to determine the connectivity, using the characteristic field H_D of the tape and the field of full penetration H^* into grains, is hindered by the fact that the demagnetizing effect of grains and thus the relationship between H^* and J_c is not sufficiently known. We found that even in high quality monofilamentary Bi-2223/Ag tapes the connectivity is very low. The largest possible value for the connectivity was 3% in a tape with $J_c^{\text{trans}}(77\,\text{K},0\,\text{T})=2\times10^8\,\text{A m}^{-2}$. Using the inverse of the connectivity to estimate the range of the upper limit of J_c^{trans}, we found $8\times10^9\,\text{A m}^{-2} < \tilde{J}_c^{\text{trans}}(77\,\text{K},0\,\text{T}) < 6\times10^{10}\,\text{A m}^{-2}$ for all three Bi-2223/Ag tapes investigated. This indicated that the intragrain critical current density was about the same in all three tapes. The remarkable similarity between the remanent magnetic moments of YBCO thin-film networks of bridged squares and monofilamentary Bi-2223/Ag tapes seems to justify our definition of connectivity for Bi-2223/Ag tapes.

Quality assessment of tapes in terms of the transport critical current density, as is presently common, is complicated by the fact that both connectivity and intragrain critical current density contribute to the transport critical current density. Measuring both connectivity and transport critical current density separately further helps to elucidate the current limiting factors in Bi-2223/Ag tapes.

ACKNOWLEDGMENTS

The authors would like to thank S. X. Dou, H. K. Liu and Y. C. Guo for providing the Bi-2223/Ag tapes 1–3.

[1] M. J. Minot, W. L. Carter, J. J. Gannon, Jr., R. S. Hamilton, P. K. Miles, D. R. Parker, G. N. Riley, Jr., M. Rupich, M. Teplitsky, E. D. Thompson, and K. Zafar, Adv. Cryog. Eng. **40**, 131 (1994).

[2] K. Sandhage, G. N. Riley, Jr., and W. L. Carter, J. Met. **43**, 21 (1991).

[3] Y. Yamada, B. Obst, and R. Flükiger, Supercond. Sci. Technol. **4**, 165 (1991).

[4] H. K. Liu, Y. C. Guo, and S. X. Dou, Supercond. Sci. Technol. **5**, 591 (1992).

[5] Y. Yamada, M. Satou, S. Murase, T. Kitamura, and Y. Kamisada (unpublished).

[6] Q. Li, K. Brodersen, H. A. Hjuler, and T. Freltoft, Physica C **217**, 360 (1993).

[7] H. Kikuchi, N. Uno, S. Tanaka, T. Hara, H. Ishii, and T. Yamamoto (unpublished).

[8] P. Haldar, J. G. Hoehn, Jr., L. R. Motowidlo, U. Balachandran, and Y. Iwasa, Adv. Cryog. Eng. **40**, 313 (1994).

[9] L. N. Bulaevskii, L. L. Daemen, M. P. Maley, and J. Y. Coulter, Phys. Rev. B **48**, 13 798 (1993).

[10] D. P. Grindatto, B. Hensel, G. Grasso, H.-U. Nissen, and R. Flükiger, Physica C **271**, 155 (1996).

[11] Q. Y. Hu, H. W. Weber, H. K. Liu, S. X. Dou, and H. W. Neumüller, Physica C **252**, 211 (1995).

[12] B. Hensel, G. Grasso, and R. Flükiger, Phys. Rev. B **51**, 15 456 (1995).

[13] N. F. Heinig, R. D. Redwing, I. Fei Tsu, A. Gurevich, J. E.

Nordman, S. E. Babcock, and D. C. Larbalestier, Appl. Phys. Lett. **69**, 577 (1996).
[14] E. H. Brandt and M. Indenbom, Phys. Rev. B **48**, 12 893 (1993).
[15] J. R. Clem and A. Sanchez, Phys. Rev. B **50**, 9355 (1994).
[16] E. H. Brandt, Phys. Rev. B **55**, 14 513 (1997).
[17] R. B. Goldfarb, M. Lelental, and C. A. Thompson, in *Magnetic Susceptibility and Other Spin Systems*, edited by R. A. Hein, T. L. Francavilla, and D. H. Liebenberg (Plenum, New York, 1991), p. 49.
[18] K.-H. Müller, C. Andrikidis, H. K. Liu, and X. S. Dou, Phys. Rev. B **50**, 10 218 (1994).
[19] M. R. Cimberle, C. Ferdeghini, R. Flükiger, E. Giannini, G. Grasso, D. Marre, M. Putti, and A. S. Siri, Physica C **251**, 61 (1995).
[20] C. Reimann, O. Waldmann, P. Müller, M. Leghissa, and B. Roas, Appl. Phys. Lett. **71**, 3287 (1997).
[21] M. Polak (private communication).
[22] K.-H. Müller, C. Andrikidis, H. K. Liu, and S. X. Dou, Physica C **247**, 74 (1995).
[23] S. X. Dou (private communication).
[24] Th. Schuster, H. Kuhn, A. Weisshardt, H. Kronmüller, B. Roas, O. Eibl, M. Leghissa, and H.-W. Neumüller, Appl. Phys. Lett. **69**, 1954 (1996).